



HAL
open science

Evaluation of output connections of interleaved dc-converter stage for photovoltaic ac-module configurations

Jaime Zapata, Samir Kouro, Thierry A Meynard

► To cite this version:

Jaime Zapata, Samir Kouro, Thierry A Meynard. Evaluation of output connections of interleaved dc-converter stage for photovoltaic ac-module configurations. 13th Brazilian Power Electronics Conference and 1st Southern Power Electronics Conference (COBEP/SPEC), Nov 2015, Fortaleza, Brazil. pp.15821972, <10.1109/COBEP.2015.7420185>. <hal-03937126>

HAL Id: hal-03937126

<https://hal.science/hal-03937126v1>

Submitted on 20 Feb 2025

HAL is a multi-disciplinary open access archive for the deposit and dissemination of scientific research documents, whether they are published or not. The documents may come from teaching and research institutions in France or abroad, or from public or private research centers.

L'archive ouverte pluridisciplinaire HAL, est destinée au dépôt et à la diffusion de documents scientifiques de niveau recherche, publiés ou non, émanant des établissements d'enseignement et de recherche français ou étrangers, des laboratoires publics ou privés.



Distributed under a Creative Commons CC BY-NC 4.0 - Attribution - Non-commercial use - International License

Evaluation of output connections of interleaved dc-converter stage for photovoltaic ac-module configurations

Jaime W. Zapata¹, Samir Kouro¹, Thierry Meynard²

¹Electronics Engineering Department, Universidad Tecnica Federico Santa Maria, Valparaiso, Chile

²Institut national polytechnique de Toulouse, University of Toulouse, Toulouse, France

email: jaime.zapataa.13@sansano.usm.cl, samir.kouro@ieec.org, thierry.meynard@laplace.univ-tlse.fr

The continuous increased installation of solar photovoltaic (PV) systems have made possible the interest in their development, oriented to reach a high efficiency system. There are four traditional configurations of grid-connected PV systems depending of the size of the plant, each of them has different efficiency values due to the inherent associated problems. The large-scale PV plants have problems when the modules do not work at the same conditions, for example when some atmospheric and environmental problems are involved, it reduces the reliability of the system. The traditional small-scale PV configurations have a low efficiency due to the dc-boosting stage in order to reach the grid levels. This work presents a grid-connected PV configuration, focused in the improve of the efficiency of the traditional ac-module configuration, a flyback topology for the dc-side and, a H-bridge topology for the grid connection will be implemented.

Keywords—DC-AC power converters, DC-DC power converters, Photovoltaic systems.

I. INTRODUCTION

Photovoltaic (PV) technology is well established as a reliable and economical source of electricity, which is gaining more importance due to the increasing power demand in the world. Grid-connected converters for PV energy systems have been grouped in different configurations and, many topologies have been proposed [1]. PV converters without transformers would be the most suitable option to minimize the cost of the total system, on the other hand, the cost of the grid-connected inverter is becoming more visible in the total system price therefore, it seems that centralized converters would be a good option for PV systems [2]. However, in small-scale PV systems, the isolated converters are required, but it increase the whole converter size and the efficiency reduction with traditional configurations.

This paper is organized as follows: The alternatives of grid-connected PV system configurations are presented in section II. The traditional ac-module, the proposed configuration and the respective control scheme are presented in section III. The simulation results are shown in section IV, and finally in section V some conclusions are given.

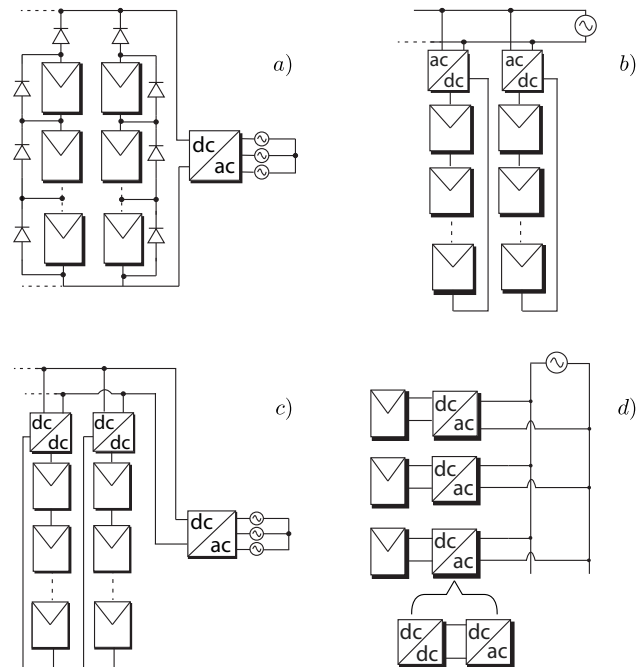


Fig. 1. Traditional grid-connected PV system configurations. a) Centralized. b) String. c) Multi-string. d) Ac-module.

II. GRID-CONNECTED PV SYSTEM CONFIGURATIONS

There are several applications where the PV systems are implemented, standalone configurations and grid-connected systems are some of them [3]. The first one is focused on the self consumption of the produced energy depending on the load specifications. The second aims to supply energy to the grid. The traditional grid-connected PV systems are centralized configuration for large-scale PV systems, multi-string configuration for large and medium-scale, string configuration for medium and small-scale systems, and ac-module configuration for small-scale systems.

Centralized configuration is oriented to large-scale PV systems. The topology is shown in Fig. 1 a). The advantages of this configurations are the simple structure and control system. However, the main drawback is the reduction of power in case

of partial shading. Therefore, the use of blocking and bypass diodes are required [4].

String configuration uses one inverter per PV string as shown in Fig. 1 b), therefore the series blocking diodes are not needed. The input voltage is high enough to avoid an elevation stage and, a separate MPPT can be applied to each string. The main drawbacks of this topology are the higher component count, this means several individual control systems and, more magnetic components if galvanic isolation is required.

Multi-string configuration is shown in Fig. 1 c). The multi-string configuration allows an individual MPPT in the dc-dc stage, a voltage elevation and isolation if is required. Therefore, this configuration is implemented in medium and, small-scale PV plants, keeping a high efficiency. Among the drawbacks there are the dc-cables losses for the connection between the dc-dc stage with the inverter converter.

Finally, the small-scale PV plants use the ac-module topology for the single-phase grid connection as shown in Fig. 1 d). It has the most flexible architecture of all configurations since one converter is connected to each PV module in order to do the MPPT. The main drawback is the low efficiency due to the voltage elevation stage required for the grid-connection.

III. MODULE INTEGRATED CONVERTERS

Module integrated converter (MIC) configuration is one of the most recent approach to grid connection for small-scale PV systems. This configuration has a dc-stage, which is formed by micro-dc converters in order to do the maximum power point tracking (MPPT), boost the dc-voltage, and provide galvanic isolation if is required and, a dc-ac inverter, which will be connected directly to the grid.

The MIC configurations are generally at cost disadvantage compared to other approaches [5], but nowadays the semiconductors and power converters development has made this configuration increasingly competitive. The small size of the converter allows a compact enclosure design that can be attached to the back of each PV module.

A. Parallel input & Parallel output connection

The commercial ac-module configuration was developed by Enphase Energy [6], currently commercialized by Siemens. The most common configuration is shown in Fig. 2 a). It works with the flyback micro-dc converter and H-bridge micro-inverter topology. The main feature of this configuration is the interleaved flyback converters connected in parallel at the input and output. With these connection the power is divided by the number of interleaved converters, enabling higher switching frequencies in the flyback semiconductor due to the lower current, and it allows a reduction in the size of the HF-transformer. This configuration works using phase shifted carriers for reference modulation stage. It allows a reduction in the current ripple both at input and output, extending the lifespan of the capacitors [7]. Because of the dc-boost stage, it configuration has the lowest efficiency compared with the other grid-connected configurations, since the voltage ratio conversion is higher between the output PV module and the grid.

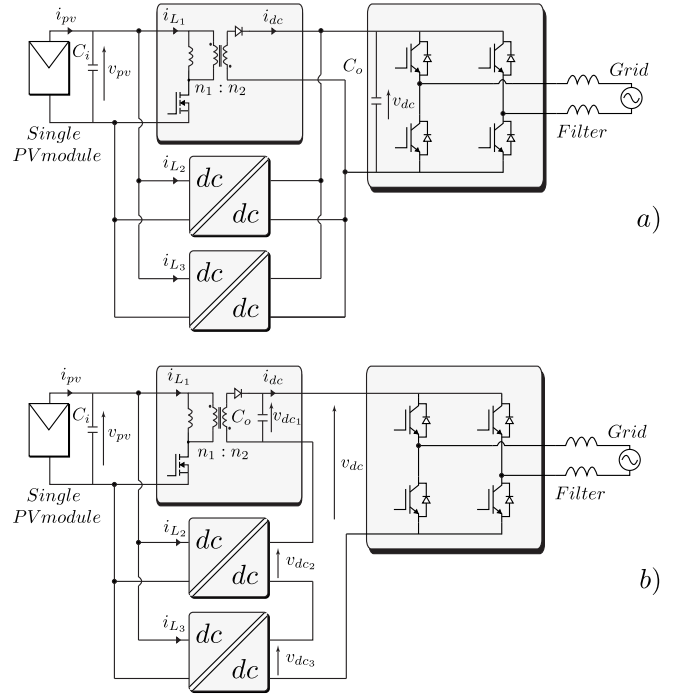


Fig. 2. Ac-module PV system based on: a) Interleaved flyback converters and H-bridge inverter [6]. b) Proposed ac-module converter.

B. Parallel input & Series output connection

The main advantage using interleaved configuration is the current distribution between the flyback converters, but the problem is the high voltage ratio in the dc-boost stage, hence the solution presented in this work is the series output connection.

This configuration is shown in Fig. 2 b). It works with the flyback micro-dc converter and H-bridge micro-inverter topology. It has the same advantages that were mentioned before due to the interleaved concept, except for the output current reduction, but considering the advantages and the results presented in the following sections, the output current ripple do not represent a considerable effect.

The series output connection allows to reach the dc-voltage level, required for the dc-ac inverter side, with a lower voltage distribution in the output of the flyback converters. For that reason, the conduction and commutation losses are lower compared with the interleaved output configuration, leading an efficiency increase. Moreover, the reduction of capacitors size is considerably due to the reduced voltage levels, hence the reduction of the converter design.

C. Flyback converter control scheme

In this work the flyback topology is implemented in the dc-dc converter stage. It presents a buck and boost feature, as shown in the equations.

$$n = \frac{n_1}{n_2} \quad (1)$$

$$\frac{V_o}{V_i} = \frac{D}{n(1-D)} \quad (2)$$

where,

- n_1 : number of turns of primary winding.
- n_2 : number of turns of secondary winding.
- V_o : output voltage.
- V_i : input voltage.
- D : duty cycle.

The main functions of the selected converter are to perform MPPT, to do a voltage elevation and to provide galvanic isolation. However the function of all dc-dc converters, is to introduce a decoupling between the output of the PV voltage and the dc-link voltage reference at the input of the grid-tied inverter. Hence the control scheme will be designed in order to achieve these aims. In literature is easily to find many dc-dc converter controllers depending of the topology and the power converter model. The new trend is to do non-linear controllers due to the converters features, however the most control structures found in practice and other power converters applications are based on linear cascaded control loops, as shown in Fig. 3 a). The outer control loop receive the voltage reference v_{pv}^* obtained from the MPPT algorithm (P&O). It is compared with the measured voltage in the input capacitor and the error is controlled using a PI controller. The output signal is the current through the input capacitor i_C^* , but the aim is to control the current through the inductor in order to remain a continuous conduction mode, therefore a feed-forward compensation loop is included, the reference given is the inductor current per each cell i_{Ln}^* . It is divided by the number of dc converters and compared with measured current of each cell. The feedback current is filtered at the switching frequency, so that it generates an imbalance in the capacitors when the filter is not included. The error signal is controlled using a PI and the output signals represent the duty cycle references, which are modulated using phase shifted carrier based PWM to reduce the input current ripple. The resulting signals S_n are used to control the dc-dc converters.

D. Single-phase voltage oriented control

The inverter stage is used to control the dc-link voltage, grid synchronization and active-reactive power control. When the control is focused in a three-phase grid connection, the dq reference frame transformation is implemented, due to it technique allows a voltage grid vector orientation and it transforms the ac values into dc-values, enabling the use of PI controllers. Nevertheless, this transformation is not possible to implement when the goal is the single-phase grid connection, but the VOC is adapted by synchronizing the grid current reference directly with the single-phase grid voltage [8].

The single-phase VOC scheme is shown in Fig. 3 b). The voltage outer loop is controlled using a PI which compares the error between the reference and the measured dc-link voltage. Notice that the implemented notch filter is important in the loop so that there is a strong second harmonic due to the rectification. The output signal of the controller is the active

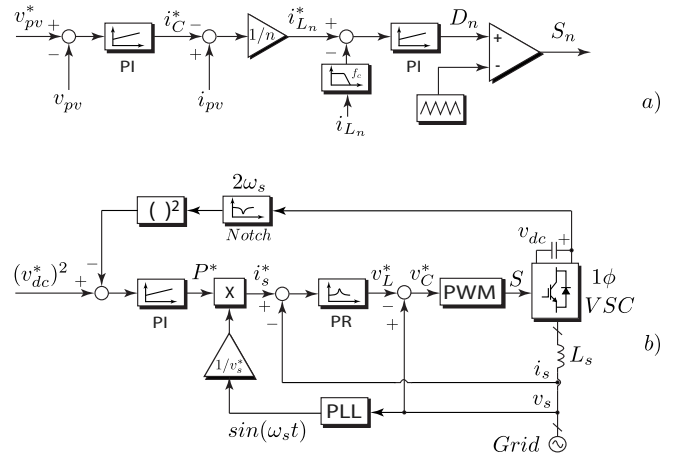


Fig. 3. Control scheme. a) Flyback control scheme. b) Single-phase voltage oriented control.

TABLE I
SIMULATION PARAMETERS

Variable	Parameter	Value
P_{pv}	PV module peak power	300 [W]
V_{mpp}	PV voltage at maximum power point	36.7 [V]
G_{stc}	Solar irradiance at STC	1000 [W/m ²]
T_{stc}	Temperature at STC	25 [°C]
V_s	Grid voltage	220 [V _{rms}]
L_s	Grid filter	10 [mH]
C_i	Input capacitor	220 [μF]
C_o	Dc-link capacitor	2200 [μF]
f_{1sw}	Dc-Ac switching frequency	3 [KHz]
f_{2sw}	Dc-Dc switching frequency	10 [KHz]

power reference (P^*) and it is divided by the grid voltage amplitude to obtain the grid current reference (i_s^*). The phase is obtained with a PLL structure and, the advantage of this, is to avoid the introduction of grid harmonics. The current reference has a sinusoidal waveform hence, a proportional resonant (PR) controller is implemented. The output signal of the controller is the grid filter inductor voltage reference (v_L^*). The converter voltage reference (V_C^*) is obtained implementing a feedforward compensation, and this signal is modulated using a PWM strategy to obtain the gate drive signal for the semiconductors.

IV. SIMULATION RESULTS

In order to validate the configuration, a comparison was made between the interleaved flyback converters connected in parallel at the input and output and the proposed one. The simulation parameters are shown in the Table I.

A. Traditional ac-module configuration

The results of the Parallel input & Parallel output connection for ac-module configuration are shown in Fig. 4. A solar irradiance change is made at $t = 1.0[s]$ in order to evaluate the dynamic behavior. In Fig. 4 a) the input voltage v_{pv} is shown. Perturb and observe (P&O) is the selected algorithm. The results shown the presence of small ripple and peaks during transitions. Fig. 4 b) shows the dc-link voltage, due to the inverter stage, the required dc voltage is at least 20% more than

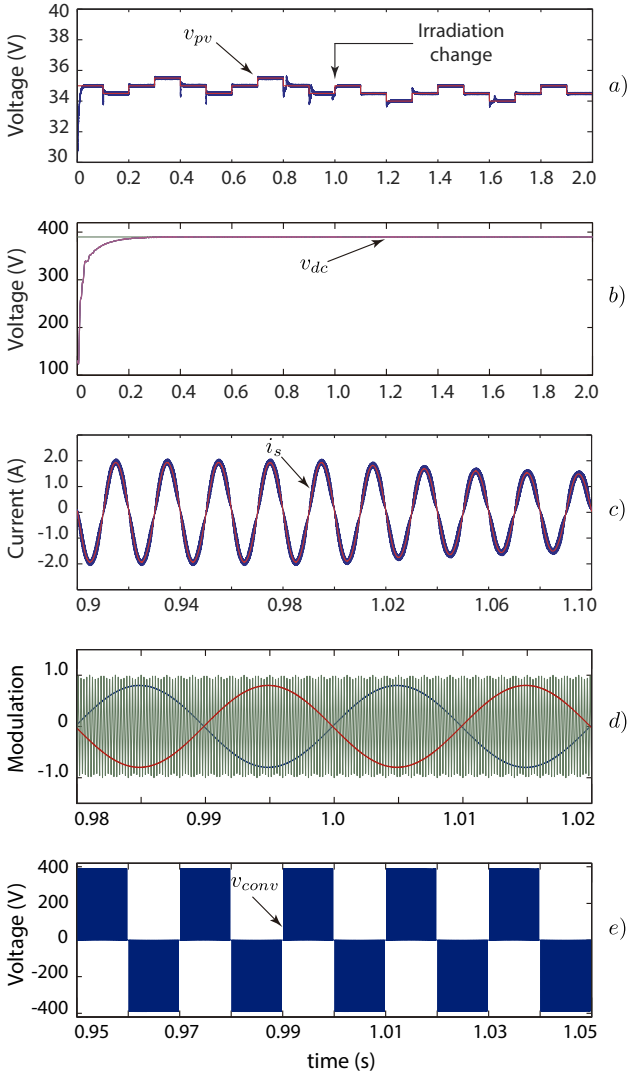


Fig. 4. Results with interleaved and series output connections.

the grid voltage. Therefore, each one of the dc-dc converters need to elevate a high voltage ratio, it is directly associated with losses. Moreover, the output capacitor must to be sized for the whole voltage, increasing the converter size. Moreover, it shows a low ripple and a good behavior in front of dynamic changes. Fig. 4 c) shows the grid current, the waveform shows a sinusoidal feature with unity power factor, the inner loop of the single-phase VOC is the responsible to achieve this aim while the outer loop keeps the dc-link in the desired level. Fig. 4 d) shows the results of modulation stage, the voltage references are sinusoidal waves, and the carrier signal has a triangular waveform. Fig. 4 e) shows the three levels in the generated voltage by the converter.

B. Proposed ac-module configuration

The results of the Parallel input & Series output connection for ac-module configuration are shown in Fig. 5. A solar irradiance change is made at $t = 1.0[s]$, as the same way that

the evaluation mentioned before. In Fig. 5 a) the input voltage v_{pv} is shown. Perturb and observe (P&O) is the selected algorithm and the results shown the lower voltage ripple and there are not peaks during the transitions. Fig. 5 b) shows the dc-link voltage and the dc-voltage generated per each cell. The capacitors start unbalanced, the trend is observed to balance itself. The main difference with the traditional ac-module configuration is that the output voltage is divided by the number of cells. Therefore, the voltage ratio elevation is lower than traditional configuration. The advantage to do this output connection is that the size of output capacitors is reduced due to the low voltage. The switching frequency in the dc-dc converter could increase, reducing the size of the magnetic components. Fig. 5 c) shows the grid current, this waveform is not different to the configuration shown before because of the inverter stage works with the full power, which is independent of the number of cells, and the control schemes are isolated between them. Fig. 5 d) shows the results of modulation stage, the voltage references are sinusoidal waves, and the carrier signal has a triangular waveform. Fig. 5 e) shows the three levels in the generated voltage by the converter.

C. Analysis of efficiency

In simulation process generally the analysis is made using ideal power electronic components however, in order to evaluate the efficiency between both connections and get the conduction and commutation losses, the model of thermal losses is implemented in each semiconductor. To analyze the diode losses, the conduction and switching losses are modeled using the following equations [9], and it is implemented in the simulation.

$$P_{cond} = v_d \cdot i_F \quad (3)$$

$$P_{sw_off} = E_{rr} \cdot f \quad (4)$$

$$P_{sw_off} = \frac{1}{4} \cdot Q_{rr} \cdot v_r \cdot f \quad (5)$$

$$Q_{rr} = \frac{1}{2} \cdot t_{rr} \cdot i_{rr} \quad (6)$$

where,

v_d : diode voltage drop.

i_F : diode forward current.

E_{rr} : reverse recovery energy losses.

f : switching frequency.

Q_{rr} : reverse recovery charge.

v_r : reverse blocking voltage.

t_{rr} : reverse recovery time.

i_{rr} : reverse recovery current.

The losses are modeled depending on the given specification for each component. It is possible to find other models based on other device database. Furthermore, it is important to notice that the turn-on switching losses are neglected so that, the energy losses are associated with the reverse recovery parameters. To analyze the mosfet and igbt losses, the model is made using the following equations.

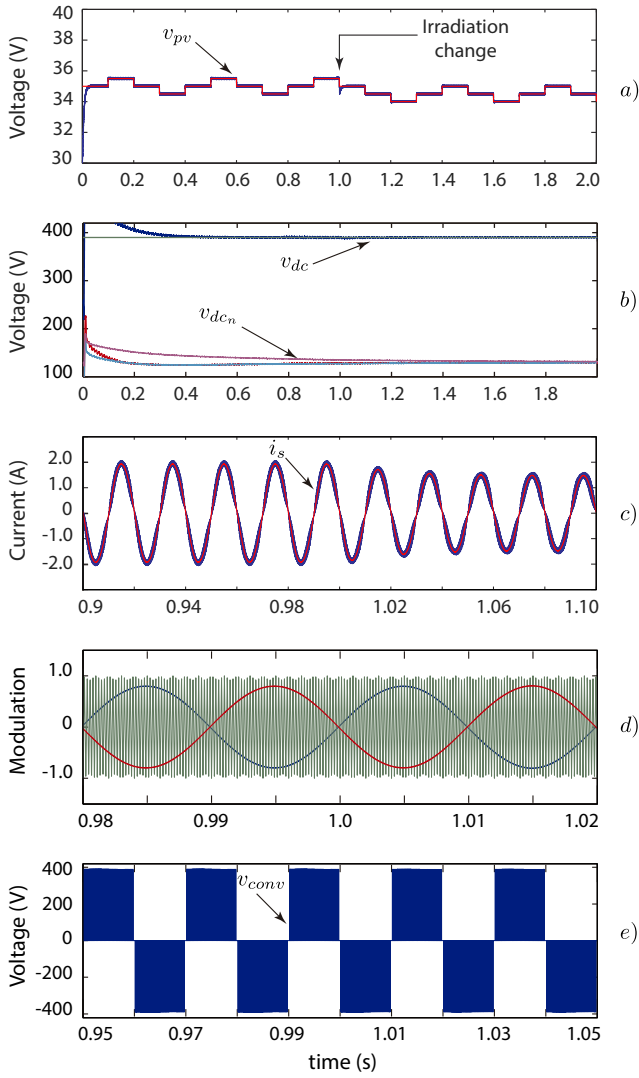


Fig. 5. Results with interleaved and series output connections.

$$P_{cond} = v_{ce,ds} \cdot i_{c,d} \quad (7)$$

$$P_{sw_{on}} = E_{on} \cdot f \quad (8)$$

$$P_{sw_{off}} = E_{off} \cdot f \quad (9)$$

$$E_{on} = v_{ce,ds} \cdot i_{c,d} \cdot t_{on} \quad (10)$$

$$E_{off} = v_{ce,ds} \cdot i_{c,d} \cdot t_{off} \quad (11)$$

where,

$v_{ce,ds}$: collector-emitter/drain-source voltage.

$i_{c,d}$: collector/drain current.

E_{on} : turn-on energy losses.

E_{off} : turn-off energy losses.

t_{on} : turn-on time.

t_{off} : turn-off time.

The energy models depends on the required accuracy. This model is based on the turn-on and turn-off times obtained from

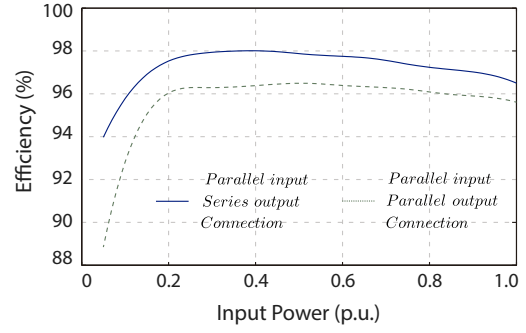


Fig. 6. Converter efficiency at different irradiance level.

the component specifications, and a simple model is presented in the following equations.

The proposed models work with a specific temperature, usually the standard test conditions are $25^{\circ}[C]$, depending on the manufacturer information. Fig. 6 shows the results at different irradiance level. The losses are directly related with the voltage ratio elevation in the dc-dc conversion stage, therefore is possible to notice that the proposed connection of micro-dc converters for ac-module configuration shows a higher efficiency.

V. CONCLUSIONS

An evaluation of two different connections of micro-dc converters for the ac-module configuration was presented in this work. The comparison was made using a single PV module, three flyback converters and a H-bridge topology for the inverter side. The traditional connection is interleaving the flyback converters at the input and output side, however it presents a lower efficiency than the proposed connection. It connection has a lower elevation ratio in the dc-side allowing a higher dc-output voltage with an increased efficiency. The results were obtained implementing models of losses and considering the conduction and switching states of the semiconductors.

VI. ACKNOWLEDGMENT

The authors acknowledge the support provided by FONDECYT Project 1151426, CONICYT/MEC Project 80130057, by AC3E (CONICYT/FB0008) of Universidad Tecnica Federico Santa Maria, and by SERC Chile (CONICYT/FONDAP/15110019).

REFERENCES

- [1] S. Kouro, J. Leon, D. Vinnikov, and L. Franquelo, "Grid-connected photovoltaic systems: An overview of recent research and emerging pv converter technology," *Industrial Electronics Magazine, IEEE*, vol. 9, no. 1, pp. 47–61, March 2015.
- [2] J. Carrasco, L. Franquelo, J. Bialasiewicz, E. Galvan, R. Guisado, M. Prats, J. Leon, and N. Moreno-Alfonso, "Power-electronic systems for the grid integration of renewable energy sources: A survey," *Industrial Electronics, IEEE Transactions on*, vol. 53, no. 4, pp. 1002–1016, June 2006.
- [3] G. Walker and J. Pierce, "Photovoltaic dc-dc module integrated converter for novel cascaded and bypass grid connection topologies - design and optimisation," in *Power Electronics Specialists Conference, 2006. PESC '06. 37th IEEE*, June 2006, pp. 1–7.

- [4] M. Calais, J. Myrzik, T. Spooner, and V. Agelidis, "Inverters for single-phase grid connected photovoltaic systems-an overview," in *Power Electronics Specialists Conference, 2002. pesc 02. 2002 IEEE 33rd Annual*, vol. 4, 2002, pp. 1995–2000.
- [5] J. Myrzik and M. Calais, "String and module integrated inverters for single-phase grid connected photovoltaic systems - a review," in *Power Tech Conference Proceedings, 2003 IEEE Bologna*, vol. 2, June 2003, pp. 8 pp. Vol.2-.
- [6] M. Fornage, "Method and Apparatus for Converting Direct Current To Alternating Current," US patent 2007/0221267A1, 2007.
- [7] S. Kouro, B. Wu, H. Abu-rub, and F. Blaabjerg, "Photovoltaic Energy Conversion systems," in *Power Electronics for Renewable Energy Systems, Transportation, and Industrial Applications*, 1st ed. IEEE/Wiley, 2014, ch. 7.
- [8] R. Teodorescu, M. Liserre, and P. Rodriguez, *Grid Converters for Photovoltaic and Wind Power Systems*. IEEE/Wiley, 2011.
- [9] G. Vazquez, T. Kerekes, A. Rolan, D. Aguilar, A. Luna, and G. Azevedo, "Losses and cmv evaluation in transformerless grid-connected pv topologies," in *Industrial Electronics, 2009. ISIE 2009. IEEE International Symposium on*, July 2009, pp. 544–548.